HHS Public Access

Author manuscript

Nature. Author manuscript; available in PMC 2016 December 30.

Published in final edited form as:

Nature. 2016 June 30; 534(7609): 697–699. doi:10.1038/nature18597.

Host-mediated sugar oxidation promotes post-antibiotic pathogen expansion

Franziska Faber[1], **Lisa Tran**[1], **Mariana X. Byndloss**[1], **Christopher A. Lopez**[1], **Eric M. Velazquez**[1], **Tobias Kerrinnes**[1], **Sean-Paul Nuccio**[1], **Tamding Wangdi**[1], **Oliver Fiehn**[2,3], **Renée M. Tsolis**[1], and **Andreas J. Bäumler**[1,*]

[1]Department of Medical Microbiology and Immunology, School of Medicine, University of California at Davis, One Shields Ave; Davis CA 95616, USA

[2]Genome Center, University of California at Davis, One Shields Ave; Davis CA 95616, USA

[3]King Abdulaziz University, Biochemistry Department, Jeddah, Saudi Arabia

Abstract

Changes in the gut microbiota may underpin many human diseases, but the mechanisms that are responsible for altering microbial communities remain poorly understood. Antibiotic usage elevates the risk of contracting gastroenteritis caused by *Salmonella enterica* serovars [1], increases the duration for which patients shed the pathogen in their feces and may on occasion produce a bacteriologic and symptomatic relapse [2,3]. These antibiotic-induced changes in the gut microbiota can be studied in mice, where the disruption of a balanced microbial community by treatment with streptomycin leads to an expansion of *S. enterica* serovars in the large bowel [4]. However, the mechanisms by which streptomycin treatment drives an expansion of *S. enterica* serovars are not fully resolved. Here we show that host-mediated oxidation of galactose and glucose promotes post-antibiotic expansion of *S. enterica* serovar Typhimurium (*S.* Typhimurium). By elevating expression of the gene encoding inducible nitric oxide synthase (iNOS) in the cecal mucosa, streptomycin treatment increased post-antibiotic availability of the oxidation products galactarate and glucarate in the murine cecum. *S.* Typhimurium utilized galactarate and glucarate within the gut lumen of streptomycin pre-treated mice and genetic ablation of the respective catabolic pathways reduced its competitiveness. Our results identify a host-mediated oxidation of carbohydrates in the gut as a novel mechanism for post-antibiotic pathogen expansion.

A recent *in silico* analysis suggests that pathways involved in galactarate uptake and catabolism are associated with *S. enterica* serovars causing gastrointestinal disease [5]. Galactarate fermentation is one of the biochemical reactions used to differentiate members

Correspondence to: Andreas J. Bäumler (ajbaumler@ucdavis.edu).

Contributions: F.F. performed bacterial growth assays, most animal expeiments and analysed the results. O.F. performed GC/MS measurements. M.X.B. performed scoring of histological sections. A.J.B., L.T., C.A.L., E.M.V., T.K. and T.W. assisted with animal experiments experiments. F.F., S.-P.N., R.M.T. and A.J.B. were responsible for the overall study design. F.F. and A.J.B. were writing the manuscript.

Competing financial Interests: The authors declare no competing financial interests

of the genus *Salmonella* into serovars. While 98.2% of serovars associated with gastrointestinal infections can ferment this carbon source, only 15.4% of serovars associated with extraintestinal disease test positive for this reaction [6] (Extended Data Fig. 1a). However, the biological significance of this association is not clear, because galactarate is a xenobiotic that is not normally produced by mammals or expected to be present within the diet. We therefore investigated the origin of galactarate in the intestine.

Consistent with the idea that galactarate is a xenobiotic, the concentration of this sugar in mouse chow was very low, as suggested by gas chromatography/mass spectrometry (GC/MS) measurements (Extended Data Fig. 1b). To investigate whether this nutrient is normally available to promote growth in mucus, we constructed a *S.* Typhimurium strain lacking the *gudT ygcY gudD STM2959* operon (*gudT-STM2959* mutant, Extended Data Fig. 1c), which encodes proteins involved in galactarate uptake and catabolism [7]. Expression of the *gudT ygcY gudD STM2959* operon in *S.* Typhimurium is induced by hydrogen, a fermentation product of the gut microbiota [8]. Deletion of galactarate utilization genes rendered *S.* Typhimurium unable to ferment galactarate and glucarate, but did not affect its ability to utilize other monosaccharides (Fig. 1a). Genetic ablation of galactarate/glucarate utilization did not reduce the fitness of *S.* Typhimurium for anaerobic growth on hog mucin as the sole carbon source, but fitness of the *gudT-STM2959* mutant was reduced compared to the wild type when galactarate or glucarate was added to the medium (Fig. 1b). These data suggested that neither the diet nor the mucus naturally contained biologically relevant quantities of a substrate for enzymes encoded by the *gudT ygcY gudD STM2959* operon.

We next investigated the contribution of the *gudT ygcY gudD STM2959* operon to post-antibiotic pathogen expansion. Treatment of mice with a single dose of streptomycin one day prior to infection (pre-treatment with streptomycin) increased recovery of the *S.* Typhimurium wild type from the colon contents of mice by approximately one order of magnitude compared to animals that had not received antibiotics ($P < 0.05$) (Fig. 1c). Genetic ablation of galactarate/glucarate utilization significantly ($P < 0.05$) reduced recovery from streptomycin pre-treated mice, but not from mice that had not received antibiotics. Genetic complementation with a plasmid carrying the cloned *gudT ygcY gudD STM2959* genes restored recovery of the *gudT-STM2959* mutant from streptomycin pre-treated mice to levels observed with the *S.* Typhimurium wild type. Collectively, these data provided genetic evidence for a contribution of the *gudT ygcY gudD STM2959* operon to post-antibiotic expansion of *S.* Typhimurium.

Preconditioning of mice with streptomycin increases the severity of *S.* Typhimurium induced colitis [9]. We therefore investigated whether the availability of galactarate/glucarate is elevated during severe colitis, a host response triggered by the action of two type III secretion systems (T3SS-1 and T3SS-2), which constitute the main virulence factors of *S.* Typhimurium [9,10]. To prevent the generation of acute intestinal inflammation, we used avirulent *S.* Typhimurium strains lacking a functional T3SS-1 (due to a mutation in *invA*) and T3SS-2 (due to a mutation in *spiB*). Streptomycin pre-treated mice were infected either with a 1:1 mixture of the wild type and a *gudT-STM2959* mutant or with a 1:1 mixture of an *invA spiB* mutant and an *invA spiB gudT-STM2959* mutant. In each competition, the galactarate/glucarate utilization-proficient strain (i.e. the wild type or the *invA spiB* mutant)

was recovered in higher numbers than the corresponding galactarate/glucarate utilization-deficient strain (i.e. the *gudT-STM2959* mutant or the *invA spiB gudT-STM2959* mutant) (Fig. 2a). However, only mice infected with a mixture of the wild type and a *gudT-STM2959* mutant developed acute intestinal inflammation (Extended Data Fig. 2 and Extended Data Tables 1 and 2). When the experiment was repeated with mice that had not received streptomycin, the presence of genes for galactarate/glucarate utilization no longer conferred a fitness advantage (Fig. 2a). To distinguish between glucarate and galactarate as possible carbon sources, we inactivated *gudD*, encoding glucarate dehydratase, or *garD*, encoding galactarate dehydratase (Extended Data Fig. 1c). During *in vitro* growth, genetic ablation of *gudD* only reduced *S.* Typhimurium fitness in medium containing glucarate, while deletion of the *garD* gene only reduced fitness in medium containing galactarate (Extended Data Fig. 1d). Both the *garD* gene and the *gudD* gene conferred a fitness advantage in streptomycin pre-treated mice (Extended Data Fig. 1e). Collectively, these data suggested that streptomycin treatment increased the availability of both glucarate and galactarate through a mechanism that was streptomycin-dependent, but independent of acute colitis triggered by *S.* Typhimurium virulence factors.

Antibiotic treatment increases the availability of sialic acid and fucose in the large intestine. It has been proposed that these monosaccharides are liberated by the resident microbiota from complex carbohydrates, a conclusion based on the observation that sialic acid and fucose are absent from cecal contents of germ-free mice [11]. We thus investigated the possibility that the gut microbiota might play a role in liberating galactarate from complex carbohydrates in the intestine. Conventional mice received either streptomycin or vehicle control by oral gavage and concentrations of galactarate and glucarate were measured in cecal contents by GC/MS four days later (Extended Data Fig. 3a and 3b). While the concentration of galactarate was low in mice that had not received antibiotics, streptomycin treatment resulted in a marked increase in the amount of galactarate present in the cecum ($P < 0.001$) (Fig. 2B). Similarly, streptomycin treatment increased ($P < 0.001$) cecal glucarate concentrations (Fig. 2c). We reasoned that if galactarate and glucarate present in streptomycin-treated mice was microbiota-liberated, then the concentrations of these sugars should be markedly reduced or absent in germ-free animals. Surprisingly, galactarate and glucarate levels measured by GC/MS in cecal contents of germ-free mice were similar or higher than those detected in conventional mice pre-treated with streptomycin (Fig. 2b and 2c). These data ruled out microbiota liberation as a possible mechanism by which streptomycin treatment elevated the availability of galactarate and glucarate in the murine large intestine.

Streptomycin treatment of mice induces elevated cecal mucosal transcript levels of *Nos2*, the gene encoding inducible nitric oxide synthase (iNOS), through an unknown mechanism [12] (Extended Data Fig. 4a). To determine whether the luminal fitness advantage conferred by galactarate/glucarate utilization genes required *Nos2* expression, streptomycin pre-treated *Nos2*-deficient mice were infected either with a 1:1 mixture of the *S.* Typhimurium wild type and a *gudT-STM2959* mutant or with a 1:1 mixture of an *invA spiB* mutant and an *invA spiB gudT-STM2959* mutant. Remarkably, in each experiment the luminal fitness advantage conferred by galactarate/glucarate utilization genes after streptomycin treatment was abrogated in *Nos2*-deficient mice (Fig. 2a). These data suggested that the *Nos2* gene was

necessary to generate a substrate for enzymes encoded by the *gudT ygcY gudD STM2959* operon.

To determine whether the streptomycin-induced increase in the cecal galactarate and glucarate concentrations (Fig. 2b and 2c) was *Nos2*-dependent, we measured galactarate and glucarate concentrations in cecal contents from *Nos2*-deficient mice four days after streptomycin treatment by GC/MS. Strikingly, streptomycin treatment did not increase the availability of these sugars in *Nos2*-deficient mice (Fig. 2b and 2c). These data further supported the idea that generation of post-antibiotic galactarate and glucarate required an intact *Nos2* gene.

To investigate whether the fitness advantage conferred by galactarate/glucarate utilization required iNOS activity, streptomycin-treated mice (C57BL/6) received drinking water supplemented with aminoguanidine hydrochloride (AG), a specific iNOS inhibitor [13], and were infected with a 1:1 mixture of the *S.* Typhimurium wild type and a *gudT-STM2959* mutant. Inhibition of iNOS activity with AG significantly ($P < 0.05$) blunted the fitness advantage conferred by galactarate/glucarate utilization genes (Fig. 2a), suggesting that iNOS activity was required for generating galactarate and glucarate in the large intestine.

The host enzyme iNOS uses L-arginine to produce nitric oxide (NO), a reactive nitrogen species (RNS) [14]. RNS are a known catalysts in the oxidation of alcohols and aldehydes [15]. We thus hypothesized that by generating RNS, streptomycin-induced iNOS synthesis might drive an oxidation of monosaccharides, thereby yielding the oxidation products galactarate and glucarate. To investigate whether RNS might oxidize galactose and glucose to galactarate and glucarate, respectively, we used 2,2,6,6-tetramethyl piperidine-1-oxyl (TEMPO), which is a stable free nitrosyl radical that mimics the activity of RNS (reviewed in [16]). Galactose and glucose were incubated in the presence of TEMPO and a co-oxidant (NaOCl) or the co-oxidant alone. Detection by GC/MS indicated that TEMPO oxidized galactose to galactarate (Fig. 2d) and glucose to glucarate (Fig. 2e). Next, we investigated whether the monosaccharides galactose and glucose were present in cecal contents. Galactose and glucose were detected in cecal contents of conventional (C57BL/6) mice, *Nos2*-deficient mice and germ-free mice (Fig. 2f and 2g). Collectively, these data suggested that monosaccharides were present in the murine cecum and could be oxidized by RNS to yield galactarate and glucarate.

Gene clusters for the utilization of galactarate and glucarate are also present in *Escherichia coli* and other related *Enterobacteriaceae* (Fig. ED1c). Since treatment with streptomycin leads to an uncontrolled expansion of *E. coli* in the murine intestine [17], we investigated whether the underlying mechanism also involved utilization of galactarate and glucarate. To this end, we deleted the *gudDXP and garD* genes in the human *E. coli* isolate Nissle 1917 (Fig. ED1c). Deletion of the *gudDXP garD* genes rendered *E. coli* unable to grow with galactarate or glucarate as the sole carbon source, but did not affect its ability to utilize glycerate (Extended Data Fig. 5a). The *gudDXP garD* genes conferred a fitness advantage during growth of *E. coli* in the colon of streptomycin pre-treated mice, which was significantly ($P < 0.05$) diminished after treatment with the iNOS inhibitor AG (Extended Data Fig. 5b).

Here we show that by inducing the production of host-derived RNS, streptomycin treatment generates galactarate and glucarate in the gut lumen, thereby providing *S.* Typhimurium and *E. coli* with a considerable fitness advantage. Increases in galactarate and glucarate levels are also observed after treatment of mice with cefoperazone or a cocktail of vancomycin and bacitracin [18,19]. A post-antibiotic expansion of *Enterobacteriaceae* is of concern due to the recent emergence of carbapenem resistance within this group. Exposure of patients in intensive care units to broad-spectrum antibiotics is a known risk factor for acquiring an infection with carbapenem-resistant *E. coli* and *Klebsiella* isolates [20]. Our findings identify host-mediated sugar oxidation as a novel mechanism contributing to post-antibiotic expansion of *Enterobacteriaceae*.

Online Methods

Bacterial strains and growth conditions

S. Typhimurium and *E. coli* strains used in this study are listed in Extended Data Table 3. All cultures were routinely grown aerobically at 37°C in either Luria-Bertani (LB) broth (10 g/l tryptone, 5 g/l yeast extract, 10 g/l NaCl) or on LB agar plates (1.5% Difco agar) unless indicated otherwise. When necessary, antibiotics were added to the medium at the following concentrations: Nalidixic acid (Nal) 50 mg/l, Kanamycin (Km) 100 mg/l, Chloramphenicol (Cm) 30 mg/l, Carbenicillin (Carb) 100 mg/l.

Sugar fermentation assay—5 ml of fermentation broth (peptone, 10 g/l; Bromothymol blue, 0.024 g/l; final pH 7.4±0.1) supplemented with the indicated carbon source (galactarate, glucarate, glucose, galactose, mannose or rhamnose, 10g/L each) or the control broth (no sugar added) were inoculated with 10μl of an over night culture of each indicated *S.* Typhimurium strain and incubated statically at 37°C for 24 hours. Fermentation of the sugar in the broth is indicated by a color change from blue to yellow.

Anaerobic growth assays—10 ml of M9 Minimal Medium (75 g/l $Na_2HPO_4 \times 2H_2O$, 30 g/l KH_2PO_4, 5 g/l NaCl, 10 g/l NH_4Cl, 0.1 mM $CaCl_2$, 1 mM $MgSO_4$, 0.001% Thiamine) supplemented with hog mucin (0.1% w/v) or galactarate (0.04% w/v when added as sole carbon source, 0.1% w/v and 0.01% w/v when added to mucin broth) were inoculated with 2 × 10^3 CFU of each strain and incubated anaerobically at 37°C for 24 hours inside an anaerobe chamber (Bactron I Anerobic Chamber; Sheldon Manufacturing, Cornelius). Bacterial numbers were determined by plating serial ten-fold dilutions onto LB agar containing the appropriate antibiotics. The ratios of recovered wild-type and mutant bacteria after 24 hours were normalized to the ratio at 0 hours to calculate the competitive index.

Construction of plasmids

Standard cloning techniques were used to generate the plasmids used in this study. All plasmids and primers used in this study are listed in Extended Data Tables 4 and 5. PCR products were confirmed by sequencing (SeqWright Fisher Scientific, Houston). Suicide plasmids were propagated in *E. coli* DH5a λ*pir*. Plasmid pFF35 was constructed by PCR amplifying a 5′ flanking fragment of *gudT* using primers 71 and 72 and a 3′ flanking fragment *STM2959* using primers 73 and 74. The two PCR fragments were gel purified,

digested with XbaI and ligated with T4 DNA Ligase (NEB). The ligation mix served as a template for a PCR with primers 71 and 74 and the product was gel purified and cloned into pCR2.1 using the TOPO TA cloning kit (Invitrogen). The plasmid construct was confirmed by sequencing and designated pFF35. To generate a suicide plasmid for replacing the *gudT ygcY gudD STM2959* genes with a kanamycin (KSAC) cassette, the insert of plasmid pFF35 was excised using BamHI and ligated into the BamHI site of the suicide plasmid pRDH10. The resulting plasmid was digested with XbaI and ligated with a KSAC cassette generated from pBS34 by digestion with XbaI. The resulting suicide plasmid was designated pFF57.

To construct plasmids pFF62 and pFF63, respectively, chromosomal regions upstream and downstream of *gudD* and *garD* in IR715 were amplified by PCR and cloned into BamHI-digested pRDH10 using Gibson Assembly Master Mix (NEB). To construct plasmids pFF64 and pFF65, respectively, chromosomal regions upstream and downstream of the gudDXP operon and of garD from *E. coli* Nissle 1917 were amplified by PCR and cloned into BamHI digested pRDH10 using Gibson Assembly Master Mix (NEB).

For complementation of the *gudT-STM2959* mutant, the *gudT ygcY gudD STM2959* operon including its promoter region was PCR amplified using primers 92/93 and 94/95. The two PCR fragments were gel purified and cloned into BamHI digested pWSK29 using Gibson Assembly Master Mix (NEB). The complementation plasmid was verified by sequencing and designated pGUDT.

Construction of mutants in *S.* Typhimurium

All suicide plasmids were introduced into *S.* Typhimurium IR715 recipient strains by conjugation using *E. coli S17-1λpir* as the donor strain. Exconjugants were selected on LB +Nal+Cm to select for clones that had integrated the suicide plasmid. Sucrose counter-selection was performed as published previously [21]. Strains that were sucrose resistant and Cm^S were verified by PCR.

Plasmid pFF57 was introduced into FF7 and SPN487 to generate FF162 (Δ*gudT-STM2959*::Km^R) and FF217 (Δ*invA* Δ*spiB* Δ*gudT-STM2959*::Km^R), respectively. Plasmid pFF62 was introduced into AJB715 to generate FF464 (*phoN*::Km^R Δ*invA* Δ*spiB gudD*). Plasmid pFF63 was introduced into AJB715 to generate strain FF461 (*phoN*::Km^R Δ*invA* Δ*spiB garD*).

Construction of mutants in *E. coli* Nissle 1917

Suicide plasmids were introduced into *E. coli* Nissle 1917(pSW172) recipient strains by conjugation using *E. coli* S17-1λ*pir* as the donor strain. To ensure stable propagation of pSW172, all steps of the conjugation were performed at 30°C. Exconjugants were selected on LB+Carb+Cm to select for clones that had integrated the suicide plasmid. Subsequent sucrose counter-selection was performed as published previously [21]. Strains that were sucrose resistant and Cm^S were verified by PCR. If appropriate, pSW172 was cured by growing the resulting mutant strains at 37°C. Plasmids pFF64 and pFF65 were successively introduced into *E. coli* Nissle 1917(pSW172) to generate FF441 (*E. coli* Nissle 1917 *gudDXP garD*).

Generalized phage transduction

Phage P22 HT105/1 *int-201* was used for generalized transduction. A phage lysate of strain CS019 was used to transduce IR715 wild-type and the Δ*invA* Δ*spiB* mutant (SPN487) to Cm^R generating FF176 (IR715 *phoN*::Tn*10d-Cam*) and FF183 (IR715 *phoN*::Tn*10d-Cam* Δ*invA* Δ*spiB*), respectively. Transductants were cleaned from phage contaminations on Evans blue-Uranine (EBU) agar plates and tested for phage sensitivity by cross-streaking against P22 H5. The strains were verified by PCR to be *phoN*::Tn*10d-Cam*.

Animal experiments

No statistical methods were used to predetermine sample size. The experiments were not randomized. The investigators were blinded to allocation of mice for assessment of histopathology and readouts of inflammation. All animal experiments were approved by the Institutional Animal Care and Use Committees at the University of California, Davis. Female C57BL/6J wild-type and *Nos2*-deficient mice (B6.129P2-*Nos2*^{tm1Lau}/J) aged 9-12 weeks were obtained from The Jackson Laboratory (Bar Harbor). Mice were pre-treated with an oral dose of 20 mg streptomycin or sterile water 24 hours before infection with *S.* Typhimurium or *E. coli* Nissle 1917, respectively. For single infections with *Salmonella*, mice were inoculated intra-gastrically with 2×10^8 CFU of the indicated *S.* Typhimurium strains. For competitive infections, mice were inoculated with a 1:1 mixture of each indicated strain. For infection with *E. coli* Nissle 1917, mice were infected with with 2×10^9 CFU of a 1:1 mixture of the indicated strains. In some experiments, dinking water was supplemented with aminoguanidine hydrochloride (1 mg/ml). Mice were euthanized 4 days after infection. The colon contents were collected for enumeration of bacterial numbers, the distal cecum was collected for histopathology scoring. Bacterial numbers were determined by plating serial ten-fold dilutions onto LB agar containing the appropriate antibiotics. The ratio of recovered wild-type and mutant bacteria in colon contents were normalized by the ratio in the inoculum to calculate the competitive index. For measurements of sugar concentrations in cecal contents, mice received an oral dose of either 20mg Streptomycin or sterile water. Mice were euthanized 4 days after streptomycin treatment and cecal contents were snap frozen in liquid nitrogen and stored at -80°C. The distal cecal tissue was collected for RNA isolation.

Germ-free Swiss Webster mice were obtained from Taconic Farms. The mice were bred and housed under germ-free conditions inside gnotobiotic isolators (Park Bioservices, LLC). Weekly 16 S PCR and cultures were performed to evaluate the germ-free status of the mice. For experiments, male and female 6-8 weeks old mice were transferred to a biosafety cabinet and maintained in sterile cages for the duration of the experiment. Cecal contents were snap frozen in liquid nitrogen and stored at -80°C until further processing for metabolite measurements.

Quantitative real-time RT-PCR analysis

Murine cecal tissue was collected, snap frozen in liquid nitrogen and stored at -80°C. Expression analysis was performed as described previously [22]. Briefly, RNA was extracted using TRI reagent (Molecular Research Center, Cincinnati) according to the manufacturer's protocol. Isolated RNA was DNase-treated (Applied Biosystems) and cDNA was

synthesized from 1μg of RNA using TaqMan reverse transcription reagents (Applied Biosystems). Real-time PCR was performed using SYBR-Green (Applied Biosystems) and the primers listed in Table 5. The changes in mRNA levels of target genes were calculated using the comparative Ct method (Applied Biosystems) and normalized to the levels of *B2M* mRNA.

Histopathology

The distal cecal tissue was fixed in phosphate-buffered formalin and 5 μm sections of the tissue were stained with hematoxylin and eosin. Blinded scoring of tissue sections was performed by a veterinary pathologist based on the criteria listed in Extended Data Tables 1 and 2. Images were taken with a Zeiss Primo Star microscope with a 10× objective.

TEMPO-mediated oxidation of sugars

The oxidation reactions were carried out at room temperature in an open beaker fitted with a pH-meter electrode and a thermometer to monitor the reactions. The pH was kept constant at 8 by titration with a 0.5 M NaOH solution. D-Galactose (2 g) and TEMPO (16 mg, 2,2,6,6-Tetramethyl-1-piperidinyloxy, free radical, Sigma-Aldrich) were dissolved in 250 ml ultrapure water. As a control some of the oxidations were done without adding TEMPO to the reaction mixture. To start the oxidation, sodium hypochlorite solution (a total of 11 ml of 10-15 % NaClO, Sigma-Aldrich) was added at a rate not exceeding a pH of 8.0. After adding the entire NaClO solution the pH was kept at 8.0 until no further pH shift was detectable. The reaction mixture was precipitated with 3 volumes of ≥ 95 % ethanol at 4°C for 48 hrs, filtered (Whatman® qualitative filter paper, grade 602 h), washed with acetone and dried at 50°C for 10-15 hrs. The resulting powdered mixture was used as a carbon source for *in vitro* growth assays and analyzed by GC-MS for the presence of galactarate.

Measurement of sugar concentrations by GC/MS

Measurements were done at the West Coast Metabolomics Center at UC Davis as previously described [23]. 20 mg of each sample, with D-Glucose-C-d7 added as the internal standard, were extracted with 1 ml of a pre-chilled acetonitrile:isopropanol:water (3:3:2) mixture. 450μl aliquots of the supernatants were evaporated to dryness and subjected to a two-step derivatization using methoximation and trimethylsilylation. GC/MS analysis was performed using an Agilent 7890 Gas Chromatography system coupled to an Agilent 5977A Mass spectrometer. An Rtx-5Sil MS w/Integra-Guard column (30 m × 250 μm i.d., Restek), chemically bonded with a 1,4-bis(dimethylsiloxy)phenylene-dimethyl polysiloxane cross-linked stationary phase (0.25 μm film thickness) was used to separate the derivatives. Helium was used as a carrier gas at a constant flow rate of 1.2 ml/min. The GC oven temperature was programmed to increase from 50°C to 325°C at a rate of 10°C/min. The temperatures of the injector, transfer line, electron impact (EI) ion source, and quadrupole were set to 250°C, 290°C, 230°C and 150°C, respectively. The mass spectrometer was set to scan at a sampling rate of 4 and data was collected in a full scan mode (m/z 50 to 600). For quantification of sugars in the samples, a 6 point calibration curve was prepared with D-Glucose-C-d7 as internal standard. Agilent Mass Hunter quant software was used for data analysis.

Statistical Analysis

The fold-changes of ratios for bacterial numbers and mRNA levels, respectively, and values for sugar concentrations were logarithmically transformed for statistical analysis. Unpaired Student's *t*-test was used to determine whether differences between groups were statistically significant ($P < 0.05$). Error bars indicate standard error of the mean (s.e.m).

Extended Data

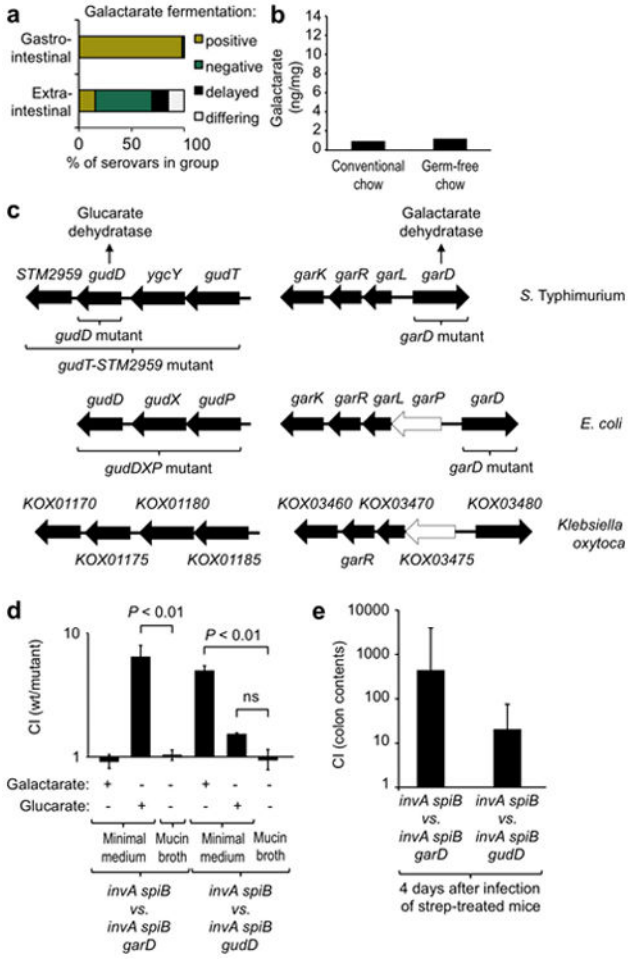

Extended Data Figure 1. Galactarate/glucarate fermentation by *S. enterica*

(**a**) One of the biochemical reactions used in the *Salmonella* serotyping scheme by Kauffman and White is the ability to ferment galactarate [6]. We divided 1,367 *S. enterica* subspecies *enterica* serovars into two groups: those associated with extraintestinal disease (i.e. serovars Typhi, Paratyphi A, Paratyphi B, Paratyphi C, Sendai, Choleraesuis, Typhisuis, Dublin, Bovismorbificans, Abortusovis, Abortusequi, Gallinarum biovar Gallinarum and Galliunarum biovar Pullorum) and those associated with human gastroenteritis (the remaining 1,354 serovars). The bar graph shows the percentages of serovars in each group that are positive, negative, delayed or differing (some isolates within the serovar are positive while others are negative) for this reaction. (**b**) Detection of galactarate in chow for conventional or germ-free mice using gas chromatography/mass spectrometry (GC/MS) (*N*

= 4). (**c**) Schematic drawing of the two gene clusters encoding proteins involved in the degradation of glucarate and galactarate in *S.* Typhimurium (ATCC14028), *E. coli* (Nissle 1917) and *Klebsiella oxytoca* (KCTC1686). Arrows indicate genes. The bracket indicates the DNA region deleted in the indicated mutants. (**d**) Minimal medium or mucin broth supplemented with the indicated carbon sources (0.1% w/v) was inoculated with a 1:1 mixture of the *S.* Typhimurium wild type and indicated mutants. CI, competitive index recovered after 24-hour incubation in an anaerobe chamber. (**e**) Streptomycin-treated C57BL6 mice ($N = 6$) were infected with a 1:1 mixture of the indicated *S.* Typhimurium strains and the CI in colon contents determined four days after infection. (**d and e**) Bars represent geometric means ± standard errors. A Student's *t*-test was applied to determine statistical significance. ns, not statistically significantly different.

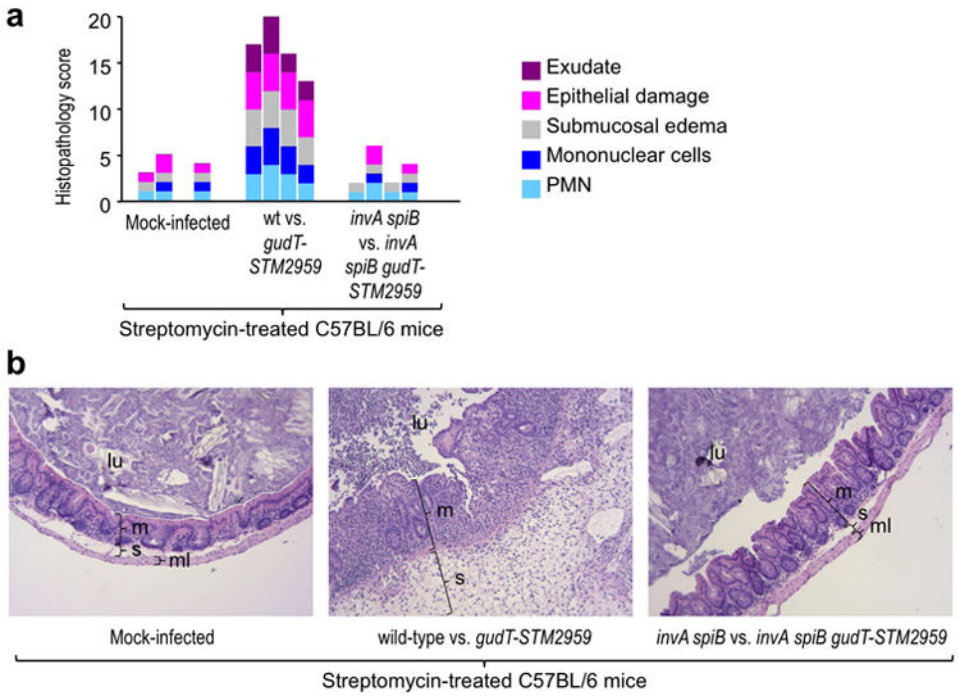

Extended Data Figure 2. Evaluation of cecal inflammation in streptomycin-treated mice 4 days after *S.* Typhimurium infection

(**A**) Streptomycin pre-treated mice were infected with the indicated strain mixtures and cecal histopathology was scored four days later for four mice per group. The criteria used for histopathology scoring are listed in Extended Data Table 4. Each bar represents data from an individual animal. (**B**) Representative images of H&E-stained cecal sections scored in panel C along with an image from a mock-infected mouse for comparison. All images were taken at the same magnification. m, mucosa; s, submucosa; ml, muscle layer; lu, lumen.

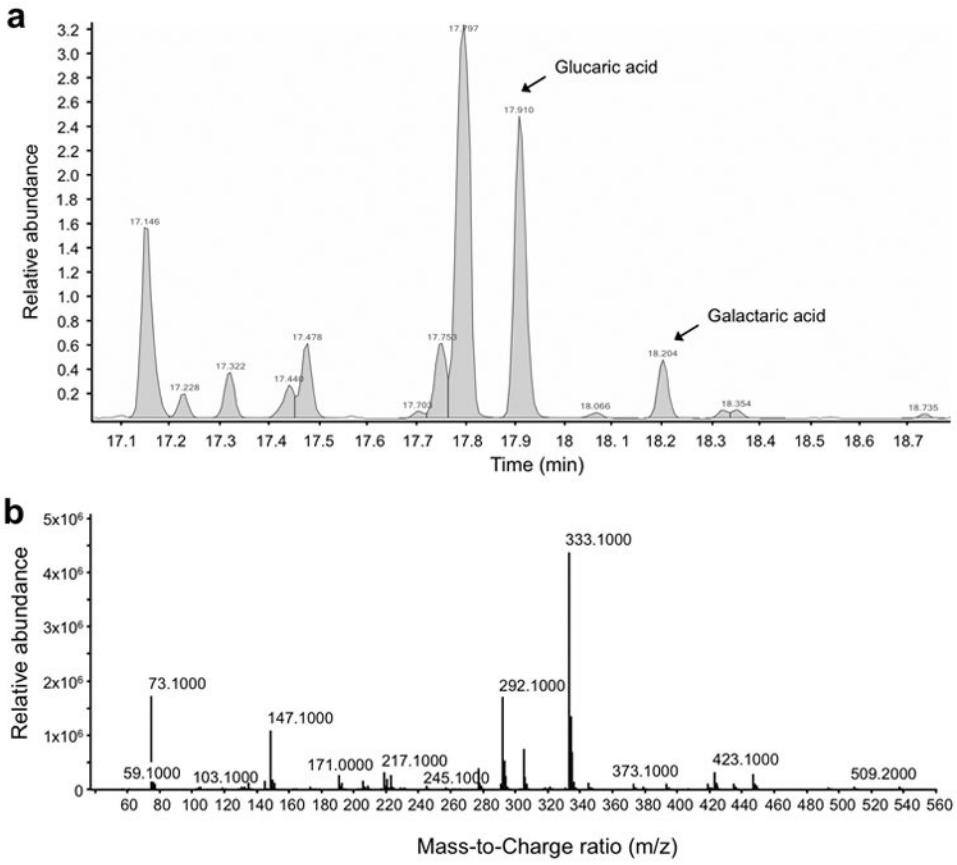

Extended Data Figure 3. Detection of galactarate and glucarate by gas chromatography/mass spectrometry (GC/MS)

(**a**) Representative GC elution profile of a cecal sample containing galactarate and glucarate (arrows). (**b**) Representative single ion monitoring scan spectrum of galactarate and glucarate.

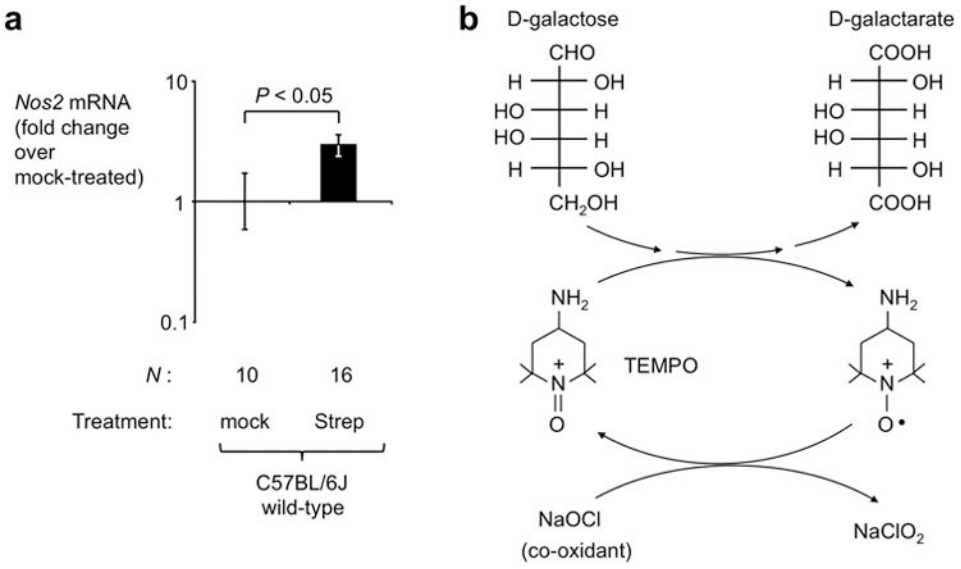

Extended Data Figure 4. Elevated *Nos2* expression leads to nitrosyl radical-mediated oxidation of galactose

(**A**) Expression levels of *Nos2* mRNA in RNA isolated from the cecal tip three days after mock-treatment (mock) or treatment of mice with streptomycin (Strep) was determined by quantitative real-time PCR. Bars represent geometric means ± standard errors. A Student's *t*-test was applied to determine statistical significance. (**B**) Schematic of the oxidation of galactose to galactarate by TEMPO. 2,2,6,6-tetramethyl piperidine-1-oxyl (TEMPO) is a stable free nitrosyl radical that can oxidize terminal alcohol and aldehyde groups to carboxyl groups [15]. Consumption of TEMPO during the redox reaction is prevented by addition of a co-oxidant (NaOCl), which regenerates the nitrosyl radical.

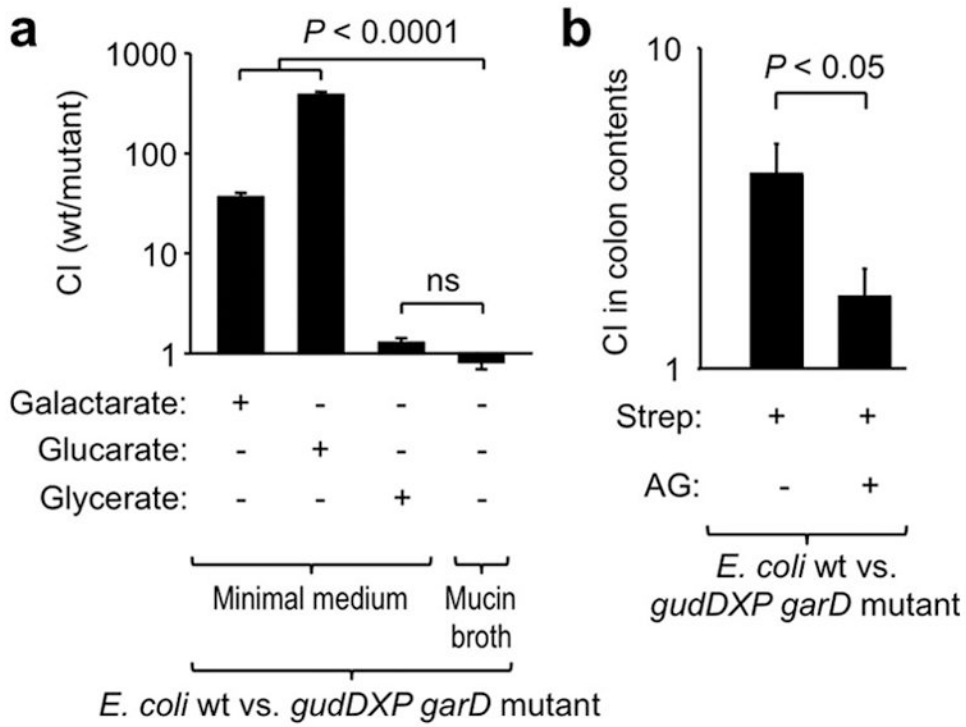

Extended Data Figure 5. Galactarate/glucarate fermentation by *E. coli*

(**a**) Minimal medium or mucin broth supplemented with the indicated carbon sources was inoculated with a 1:1 mixture of the *E. coli* wild type (wt) and a *garDXP garD* mutant. CI, competitive index recovered after 24-hour incubation in an anaerobe chamber. Growth was verified with 3 biological replicates. (**b**) Streptomycin-treated C57BL6 mice ($N = 6$) were infected with a 1:1 mixture of the indicated *E. coli* strains and received the iNOS inhibitor aminoguanidine (AG) or vehicle control. The CI in colon contents was determined four days after infection. (**a and b**) Bars represent geometric means ± standard errors. A Student's *t*-test was applied to determine statistical significance. ns, not statistically significantly different.

Extended Data Table 1

Chart indicating scoring criteria for blinded examination of H&E-stained sections from the cecum

Score	Submucosal edema	Epithelial damage	Exudate	PMN infiltration*	Mononuclear cell infiltrate*
0	No changes	No changes	No changes	No changes (0-5)	No changes (0-5)
1	Detectable (<10%)	Desquamation	Slight accumulation	6-20	5-10
2	Mild (10%-20%)	Mild erosion	Mild accumulation	21-60	10-20
3	Moderate (20%-40%)	Marked erosion	Moderate accumulation	60-100	20-40
4	Marked (>40%)	Ulceration	Marked accumulation	>100	>40

*Number of cells per high power microscopic field

Extended Data Table 2
Blinded histopathology scoring scheme

Combined score	Description
>8	Severe inflammation
6-8	Moderate inflammation
3-5	Mild inflammation
0-2	Normal

Extended Data Table 3
Bacterial strains used in this study

Designation	Genotype	Reference
E. coli		
TOP10	F- *mcrA* Δ(*mrr-hsdRMS-mcrBC*) Φ80*lacZ*ΔM15 *lacX74 recA 1 araD139* Δ(*ara - leu*)*7697 galU galK rpsL endA1 nupG*	Invitrogen
DH5a *λpir*	F- *endA1 hsdR17* (r-m+) *supE44 thi-1 recA1 gyrA relA1* Δ(*lacZYA-argF*)*U189* Φ80/ *acZ*ΔM15 λ*pir*	Lab stock
S17-1λpir	*zxx*::RP4 2-(Tet^R::Mu) (Km^R::Tn7) λ*pir*	Lab stock
Nissle 1917	Wild-type strain (O6:K5:H1)	[24]
FF441	Nissle 1917 *gudDXP garD*	This Study
Salmonella		
ATCC 14028	Wild-type isolate of *S. enterica* serovar Typhimurium	ATCC
IR715	Nalidixic acid-resistant derivative of ATCC14028	[25]
CS019	ATCC 14028 *phoN*::Tn *10d-Cam*	[26]
SPN487	IR715 Δ*invA* Δ*spiB*	[27]
FF176	IR715 *phoN*::Tn *10d-Cam*	This Study
AJB715	IR715 *phoN*::Km^R	[28]
FF183	IR715 *phoN*::Tn *10d-Cam* Δ*invA* Δ*spiB*	This Study
FF162	IR715 *gudTygcYgudDSTM2959*::Km^R	This Study
FF461	IR715 *phoN*::Km^R Δ*invA* Δ*spiB garD*	This Study
FF464	IR715 *phoN*::Km^R Δ*invA* Δ*spiB gudD*	This Study
FF217	IR715 Δ*invA* Δ*spiB* Δ*gudTygcYgudDSTM2959*::Km^R	This Study

Extended Data Table 4
Plasmids used in this study

Designation	Relevant Characteristics	Reference
pCR2.1	Cloning vector, Carb^R, Km^R	Invitrogen
pRDH10	*ori*(R6K) *mobRP4 sacRB* Tet^R Cm^R	Lab stock
pBS34	pBluescript II KS+, KSAC cassette, Carb^R, Km^R	[29]
pWSK29	Cloning vector, *ori*(pSC101) Carb^R	Lab stock

Designation	Relevant Characteristics	Reference
pFF35	5′ and 3′ flanking regions of *gudTygcYgudDSTM2959* operon in pCR2.1, $Carb^R$, Km^R	This Study
pFF57	KSAC cassette flanked by up-/downstream regions of the *gudTygcYgudDSTM2959* operon in pRDH10; Cm^R, Km^R	This Study
pSW172	ori(R101) *repA*101ts $Carb^R$	30
pCAL61	ori(R101) Kan^R $Strep^R$	12
pCAL62	ori(R101) $Carb^R$ $Strep^R$	12
pFF62	Up-/down stream regions of gudD from IR715 in pRDH10	This Study
pFF63	Up-/downstream regions of garD from IR715 in pRDH10	This Study
pFF64	Up-/downstream regions of the gudDXP operon from EcN in pRDH10	This Study
pFF65	Up-/downstream regions of garD from EcN in pRDH10	This Study
pGUDT	*gudTygcYgudDSTM2959* operon under the control of its native promoter in pWSK29; $Carb^R$	This Study

Extended Data Table 5
Primers used in this study

Deletion of gudTygcYgudDSTM2959	
Primer	**Sequence** *
71	5′-GGATCCTCTGAACCGCTGCTAATGG-3′
72	5′-TCTAGAGTTACGCTGAGTTGTAGG-3′
73	5′-TCTAGAGTAGGGAATCAGAGATAACG-3′
74	5′-GGATCCAGGGAGATACGCATAATGG-3′
Deletion of gudD in IR715	
116	**CACACCCGTCCTGTG**CTCAACATGCACGATTCG
117	**CGATCTCC**CGATGTTTACCCATGTTG
118	**TAAACATCG**GGAGATCGAACGTTTGTAAG
119	**GCGTCCGGCGTAGAG**GAGCTTGACTGGGAACAG
Deletion ofgarD in IR715	
112	**CACACCCGTCCTGTG**CTGAAATCAGAATGGGTC
113	**TCACAGGT**CGGAATATGTTCAGTCAGTTC
114	**CATATTCCG**ACCTGTGACCTGATCTATTCTG
115	**GCGTCCGGCGTAGAG**ATTGTCGCAAGGCTTCAC
Complementation of gudTygcYgudDSTM2959	
92	5′-**TCCTGCAGCCCGGGG**CTTGCGTTGCCAGTAAGC-3′
93	5-**TTAACGCACCATGCAAG**GAC-3′
94	5′-**CTTGCATGGTGCGTTAA**GTC-3′
95	5′-**CGCTCTAGAACTAGTG**ATCCGGCCTACAACTCAGC-3′
Deletion of gudDXP operon in E. coli Nissle 1917	
136	**CACACCCGTCCTGTG**CTGTGTTTATGCCGGATG
137	**CCGGTTCG**TTCCCTGGCGATGTTTAC

138	**CCAGGGAA**CGAACCGGCAATAGAAAGC	
139	**GCGTCCGGCGTAGAG**TTTGCCTGGAGTCAAGCG	
Deletion ofgarD in E. coli Nissle 1917		
235	**CACACCCGTCCTGTGT**GGCCAACATCAAAATCAG	
236	**CACCGGTG**GTTCGGGTATTTCGGTAG	
237	**ACCCGAAC**CACCGGTGACCTGATTTC	
238	**GCGTCCGGCGTAGAG**GCCAGCGACAAGTTTCTTTC	
Quantitative real-time RT-PCR		
Organism	**Target**	**Sequence**
Mus musculus	*B2M*	5′-GGTCTTTCTGGTGCTTGTCTCA-3′
		5′-GTTCGGCTTCCCATTCTCC-3′
Mus musculus	*Nos2*	5′-TTGGGTCTTGTTCACTCCACGG-3′
		5′-CCTCTTTCAGGTCACTTTGGTAGG-3′

* restriction enzyme sites are underlined, overlapping sequences for Gibson Assembly are in bold

Acknowledgments

This work was supported by Public Health Service Grants OD010931 (E.M.V.), AI060555 (S.-P.N.), AI096528 (A.J.B.), AI109799 (R.M.T), AI112241 (C.A.L.), AI112258 (R.M.T), AI112445 (A.J.B.), U24 DK097154 (O.F.), AI112949 (A.J.B.) and AI114922 (A.J.B.).

Literature

1. Pavia AT, et al. Epidemiologic evidence that prior antimicrobial exposure decreases resistance to infection by antimicrobial-sensitive Salmonella. J Infect Dis. 1990; 161:255–260. [PubMed: 2299207]
2. Nelson JD, Kusmiesz H, Jackson LH, Woodman E. Treatment of Salmonella gastroenteritis with ampicillin, amoxicillin, or placebo. Pediatrics. 1980; 65:1125–1130. [PubMed: 7375236]
3. Aserkoff B, Bennett JV. Effect of antibiotic therapy in acute salmonellosis on the fecal excretion of salmonellae. The New England journal of medicine. 1969; 281:636–640. [PubMed: 4897014]
4. Bohnhoff M, Drake BL, Miller CP. Effect of streptomycin on susceptibility of intestinal tract to experimental Salmonella infection. Proc Soc Exp Biol Med. 1954; 86:132–137. [PubMed: 13177610]
5. Nuccio SP, Baumler AJ. Comparative analysis of Salmonella genomes identifies a metabolic network for escalating growth in the inflamed gut. MBio. 2014; 5:e00929–00914. DOI: 10.1128/mBio.00929-14 [PubMed: 24643865]
6. Kelterborn, E. Kauffmann-White-Schema (1989). Bundesgesundheitsamt; Berlin: 1992. p. 1-171.
7. Lamichhane-Khadka R, Frye JG, Porwollik S, McClelland M, Maier RJ. Hydrogen-stimulated carbon acquisition and conservation in Salmonella enterica serovar Typhimurium. Journal of bacteriology. 2011; 193:5824–5832. DOI: 10.1128/JB.05456-11 [PubMed: 21856852]
8. Lamichhane-Khadka R, Benoit SL, Maier SE, Maier RJ. A link between gut community metabolism and pathogenesis: molecular hydrogen-stimulated glucarate catabolism aids Salmonella virulence. Open Biol. 2013; 3:130146. [PubMed: 24307595]
9. Barthel M, et al. Pretreatment of mice with streptomycin provides a Salmonella enterica serovar Typhimurium colitis model that allows analysis of both pathogen and host. Infection and immunity. 2003; 71:2839–2858. [PubMed: 12704158]

10. Tsolis RM, Adams LG, Ficht TA, Baumler AJ. Contribution of Salmonella typhimurium virulence factors to diarrheal disease in calves. Infection and immunity. 1999; 67:4879–4885. [PubMed: 10456944]
11. Ng KM, et al. Microbiota-liberated host sugars facilitate post-antibiotic expansion of enteric pathogens. Nature. 2013; 502:96–99. DOI: 10.1038/nature12503 [PubMed: 23995682]
12. Spees AM, et al. Streptomycin-Induced Inflammation Enhances Escherichia coli Gut Colonization Through Nitrate Respiration. mBio. 2013; 4:e00430–00413. DOI: 10.1128/mBio.00430-13 [PubMed: 23820397]
13. Stefanovic-Racic M, et al. Comparison of the nitric oxide synthase inhibitors methylarginine and aminoguanidine as prophylactic and therapeutic agents in rat adjuvant arthritis. J Rheumatol. 1995; 22:1922–1928. [PubMed: 8991992]
14. Palmer RM, Ashton DS, Moncada S. Vascular endothelial cells synthesize nitric oxide from L-arginine. Nature. 1988; 333:664–666. DOI: 10.1038/333664a0 [PubMed: 3131684]
15. de Souza M. The use of TEMPO (2,2,6,6-tetramethylpiperidine-N-oxyl) for the oxidation of primary and secondary alcohols. QUIMICA NOVA. 2004; 27:287–292.
16. Sheldon RA, Arends IWCE. Organocatalytic oxidations mediated by nitroxyl radicals. Adv Synth Catal. 2004; 346:1051–1071. DOI: 10.1002/Adsc.200404110
17. Ozawa A, Freter R. Ecological Mechanism Controlling Growth of Escherichia Coli in Continuous Flow Cultures and in the Mouse Intestine. J Infect Dis. 1964; 114:235–242. [PubMed: 14183395]
18. Theriot CM, et al. Antibiotic-induced shifts in the mouse gut microbiome and metabolome increase susceptibility to Clostridium difficile infection. Nat Commun. 2014; 5:3114. [PubMed: 24445449]
19. Hwang I, et al. Alteration of gut microbiota by vancomycin and bacitracin improves insulin resistance via glucagon-like peptide 1 in diet-induced obesity. FASEB J. 2015; 29:2397–2411. DOI: 10.1096/fj.14-265983 [PubMed: 25713030]
20. Tangden T, Giske CG. Global dissemination of extensively drug-resistant carbapenemase-producing Enterobacteriaceae: clinical perspectives on detection, treatment and infection control. J Intern Med. 2015; 277:501–512. DOI: 10.1111/joim.12342 [PubMed: 25556628]

References for Online Materials and Methods

21. Lawes M, Maloy S. MudSacI, a transposon with strong selectable and counterselectable markers: use for rapid mapping of chromosomal mutations in Salmonella typhimurium. Journal of bacteriology. 1995; 177:1383–1387. [PubMed: 7868615]
22. Winter SE, et al. Contribution of flagellin pattern recognition to intestinal inflammation during Salmonella enterica serotype typhimurium infection. Infection and immunity. 2009; 77:1904–1916. DOI: 10.1128/IAI.01341-08 [PubMed: 19237529]
23. Fiehn O, et al. Quality control for plant metabolomics: reporting MSI-compliant studies. Plant J. 2008; 53:691–704. DOI: 10.1111/j.1365-313X.2007.03387.x [PubMed: 18269577]
24. Grozdanov L, et al. Analysis of the genome structure of the nonpathogenic probiotic Escherichia coli strain Nissle 1917. Journal of bacteriology. 2004; 186:5432–5441. DOI: 10.1128/JB.186.16.5432-5441.2004 [PubMed: 15292145]
25. Stojiljkovic I, Bäumler AJ, Heffron F. Ethanolamine utilization in Salmonella typhimurium: nucleotide sequence, protein expression, and mutational analysis of the cchA cchB eutE eutJ eutG eutH gene cluster. Journal of bacteriology. 1995; 177:1357–1366. [PubMed: 7868611]
26. Miller SI, Kukral AM, Mekalanos JJ. A two-component regulatory system (phoP phoQ) controls Salmonella typhimurium virulence. Proceedings of the National Academy of Sciences of the United States of America. 1989; 86:5054–5058. [PubMed: 2544889]
27. Rivera-Chavez F, et al. Salmonella uses energy taxis to benefit from intestinal inflammation. PLoS pathogens. 2013; 9:e1003267. [PubMed: 23637594]
28. Kingsley RA, et al. Molecular and phenotypic analysis of the CS54 island of Salmonella enterica serotype typhimurium: identification of intestinal colonization and persistence determinants. Infection and immunity. 2003; 71:629–640. [PubMed: 12540539]

29. Raffatellu M, et al. Lipocalin-2 resistance confers an advantage to Salmonella enterica serotype Typhimurium for growth and survival in the inflamed intestine. Cell host & microbe. 2009; 5:476–486. DOI: 10.1016/j.chom.2009.03.011 [PubMed: 19454351]

30. Winter SE, et al. Host-derived nitrate boosts growth of E. coli in the inflamed gut. Science. 2013; 339:708–711. DOI: 10.1126/science.1232467 [PubMed: 23393266]

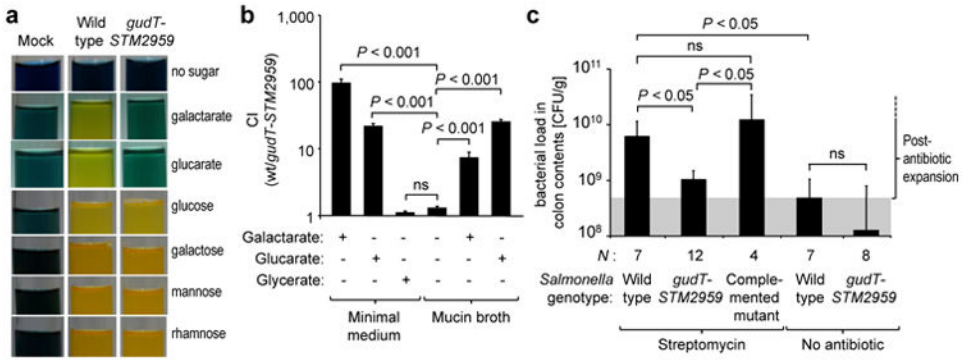

Fig. 1. The operon for galactarate utilization contributes to post-antibiotic expansion of *S.* Typhimurium

(**a**) The ability of the indicated *S.* Typhimurium strains to ferment the indicated monosaccharides was detected using a pH indicator. (**b**) Minimal medium or mucin broth supplemented with the indicated carbon sources (0.1 % w/v) was inoculated with a 1:1 mixture of the *S.* Typhimurium wild type and the *gudT-STM2959* mutant. CI, competitive index recovered after 24-hour incubation in an anaerobe chamber. (**a** and **b**) Growth was verified with 3 biological replicates. (**c**) Groups of streptomycin pre-treated or mock-treated (no antibiotic) mice (C57BL/6) received the indicated *S.* Typhimurium strains by oral gavage and bacteria were recovered from colon contents four days later. Grey shading indicates average colonization levels of the *S.* Typhimurium wild type in mice that had not received antibiotics. Wild type, IR715; *gudT-STM2959* mutant, FF162; complemented mutant, FF162(pGUDT); *N* indicates number of individual mice. (**b-c**) Bars represent geometric means ± s.e.m. A Student's *t*-test was applied to determine statistical significance. ns, not statistically significantly different.

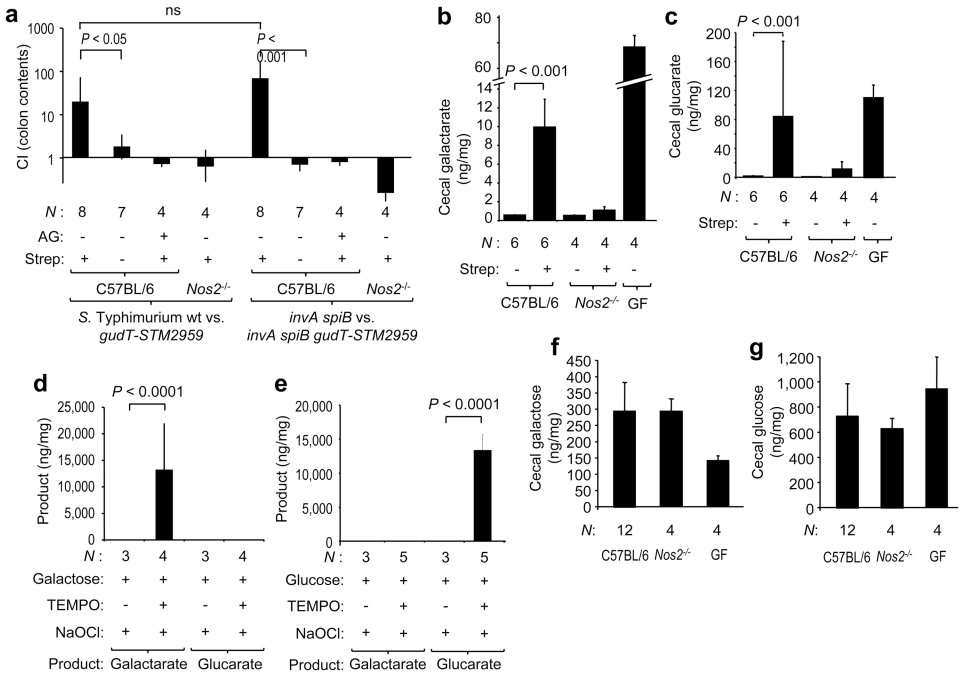

Fig. 2. Post-antibiotic generation of galactarate and glucarate is *Nos2*-dependent

(**a**) Groups of wild type (C57BL/6) mice, streptomycin (Strep) pre-treated C57BL/6 mice or streptomycin pre-treated *Nos2*-deficient (*Nos2*$^{-/-}$) mice were infected with the indicated strain mixtures and received drinking water with or without aminoguanidine hydrochloride (AG) supplementation. The competitive index (CI) in colon contents was determined four days later. (**b and c**) Groups of C57BL/6 mice, congenic *Nos2*$^{-/-}$ mice or germ-free Swiss Webster mice were mock-treated or treated with streptomycin and galactarate concentrations (**b**) or glucarate concentrations (**c**) in cecal contents were determined by gas chromatography/mass spectrometry (GC/MS) four days later. (**d and e**) Oxidation of galactose to galactarate (**d**) or glucose to glucarate (**e**) by the stable nitrosyl radical TEMPO was determined by GC/MS. (**f and g**) Concentrations of galactose (**f**) or glucose (**g**) in cecal contents of the indicated mouse strains were determined by gas chromatography/mass spectrometry (GC/MS). *N* indicates number of individual mice (**a-c and f-g**) or number of independent oxidation reactions (**d-e**). (**a-g**) Bars represent geometric means ± standard errors. A Student's *t*-test was applied to determine statistical significance. ns, not statistically significantly different.